Available online at www.sciencedirect.com
SCIENCE DIRECT®
Physica C 404 (2004) 410–414
PHYSICA C
www.elsevier.com/locate/physc

Flux flow anisotropy in superconducting films with a rectangular array of holes

Marco S. Welling [a,*], Rinke J. Wijngaarden [a], Christof M. Aegerter [a], Roger Wördenweber [b], Peter Lahl [b]

[a] Division of Physics and Astronomy, Vrije Universiteit, FEW, De Boelelaan 1081, 1081HV Amsterdam, The Netherlands
[b] Institut für Schichten und Grenzflächen (ISG), Forschungszentrum Jülich, Germany

Abstract

We present a study of the flux penetration in $YBa_2Cu_3O_{7-x}$ thin films with a rectangular array of holes (anti-dots), visualizing the magnetic flux density using an advanced magneto-optical technique. Flux penetration patterns are explained by a simple model based on the channeling of vortices along rows of holes. In simulations this was found to lead to a large anisotropy ~60 of the critical current. However, our experimental anisotropy of 1.30(5) is much smaller. We discuss possible reasons for this discrepancy.

PACS: 74.78.Bz; 74.25.Op; 74.25.Qt
Keywords: YBCO; Magneto-optics; Anti-dots

1. Introduction

In a previous publication [1] some of us showed that, while the macroscopic resistivity of a copper disk remains isotropic if it is perforated with a square array of small holes or 'anti-dots', a superconductor behaves quite differently: a four-fold symmetry in the critical current is created. This symmetry cannot be described by the usual concept of a resistivity tensor, but is a consequence of the non-linearity, and hence the non-additivity, of currents in superconductors. In this paper we investigate the effect of a *rectangular* array of anti-dots enabling a more detailed determination of the influence of the anti-dots on the critical current and the flux penetration.

Magnetic flux penetration in a superconductor takes place in the form of quantized vortices that may interact with defects such as anti-dots. The pinning of vortices on defects has gained renewed interest because of the possibility of noise reduction in SQUIDS [2] and because of its fundamental importance. The effect of periodic pinning arrays on flux penetration has been studied recently in square samples (where an accurate determination of the angular dependence of the critical current is not possible) magneto-optically [3,4] and also in numerical simulations by Reichhardt et al. [5]. In these simulations on samples with square and rectangular pinning arrays, maxima in the pinning

* Corresponding author.
E-mail address: welling@nat.vu.nl (M.S. Welling).

0921-4534/$ - see front matter © 2004 Elsevier B.V. All rights reserved.
doi:10.1016/j.physc.2003.11.026

force are observed when the vortex lattice is commensurate with the pinning lattice, in nice agreement with experimental results [6,7]. In addition, for a ratio of 2 between the *a*- and *b*-anti-dot lattice vectors, the pinning force is found to have a large anisotropy of ~60.

In this paper we study the magnetic flux dynamics in $YBa_2Cu_3O_{7-x}$ thin films [8] with a rectangular anti-dot array with lattice vectors of 10 and 20 μm. The magnetic flux density is measured using an advanced magneto-optical (MO) technique [9]. We determine the anisotropy and angular dependence of the critical current and present a simple geometrical model, which fits the experimental results.

2. Experimental

The samples consist of 200 nm thick $YBa_2Cu_3O_{7-x}$ (YBCO) thin films epitaxially grown on a $SrTiO_3$ substrate by laser ablation [8]. Circular anti-dots (holes of 2.5 μm in diameter), are etched into the superconductor using e-beam lithography and ion beam etching. The anti-dot lattice has a unit cell of 10×20 μm, as shown in Fig. 1. The circular sample has a diameter of 1.7 mm. A protective gold layer is deposited on top of the sample.

We measure the local magnetic flux density B_z directly above the superconducting sample using a MO set-up [9] by detecting the polarization change in a Bi-substituted ferrite–garnet film with in-plane magnetization vector and large Faraday effect (typically 0.06 deg/mT). We mount this 'indicator' on top of the sample and place the assembly in our specially built cryogenic polarization microscope, which fits into the variable temperature insert of an Oxford Instruments 1-T magnet system.

Experiments are performed at 4.2 and 60 K after zero field cooling (ZFC). We do not present the 60 K results here since the behavior at 60 K is qualitatively identical to the 4.2 K result (i.e. the anisotropy does practically not change, in contrast to Ref. [3]), while the lower j_c at 60 K increases the uncertainty in quantitative determinations. The externally applied magnetic field is perpendicular to the sample and indicator surface. We perform

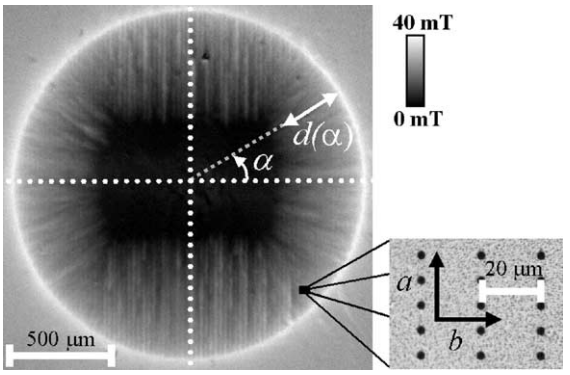

Fig. 1. Measured local magnetic flux density B_z in a disk shaped $YBa_2Cu_3O_{7-x}$ thin film containing a rectangular anti-dot array after zero field cooling to 4.2 K and subsequently applying a field of 23 mT. Anti-dots are holes with a diameter of 2.5 μm and the anti-dot lattice has a unit cell of 10×20 μm. Flux flow preferentially takes place along anti-dot channels parallel to the lattice vectors *a* and *b*. The inset indicates the anti-dot array. The flux front penetration distance, $d(\alpha)$, is measured from the circle edge toward the circle center and describes the front separating the Shubnikov phase (where vortices have penetrated; bright) from the Meissner phase (vortex free; black).

full hysteresis loops to 95 mT in steps of 0.5 mT starting from zero, using a constant sweep rate of 0.1 mT/s between steps. After every field step, the flux distribution in the sample is relaxed for 7 s after which a MO image is acquired. Our camera has 782×582 pixels and the exposure time is 800 ms. The spatial resolution is such that the width of a square pixel equals 3.3 μm.

3. Results

Shown in Fig. 1 is a MO image of the flux penetration in the sample after ZFC to 4.2 K and subsequently applying a magnetic field of 23 mT. The flux front is the border of the black Meissner area. Current flows in the band between the Meissner phase and the sample edge. Defining $d(\alpha)$ as the width of this band (see Fig. 1), we observe a variation of d with the polar angle α. Since current sources and sinks are absent in the sample, the current is continuous and the current density $j(\alpha)$ is inversely proportional to $d(\alpha)$.

Looking in more detail to Fig. 1, we observe vertical and horizontal parallel streaks in the

current carrying band due to channeling of vortices along rows of anti-dots. It seems [1] that vortices move into the sample only along the anti-dot array lattice vector closest to the Lorentz force direction (which is initially perpendicular to the sample edge).

We first focus on a quantitative analysis of the measured flux front penetration distance, $d(\alpha)$, as defined above in Fig. 1. Using mirror planes, we average the four quadrants thereby obtaining a more accurate determination of $d(\alpha)$. In Fig. 2a, we show the observed flux fronts for various values of the externally applied magnetic field.

From the $d(\alpha)$ curves of Fig. 2a, we calculate the critical current anisotropy $A = j_c\ (0°)/j_c(90°) = d(90°)/d(0°)$ as a function of external field, see Fig. 3.

In Fig. 4 we show the angular dependence of the critical current density at 50 mT (on the plateau in Fig. 3).

While numerical simulations [5] give $\sim$60 for the anisotropy $j_c(0°)/j_c(90°)$, we find the much lower value 1.30(5). Possibly this is caused by vortices jumping from one row of anti-dots to an adjacent one (channel switching), hence lowering the anisotropy. It is well known that $YBa_2Cu_3O_{7-x}$ samples have strong natural pinning centers distributed randomly in space. Such pinning centers may promote channel switching. Another (more important) reason for the discrepancy may be the large difference in parameters such as size of and distance between anti-dots compared to the scale of a vortex.

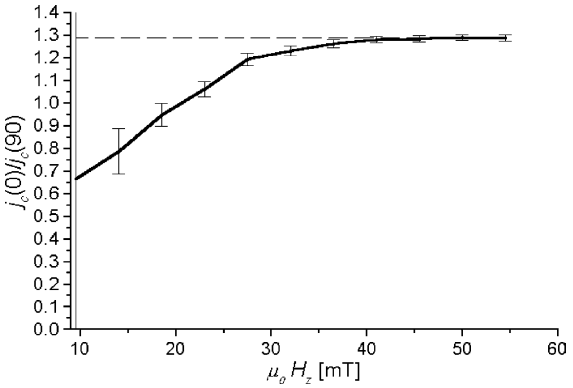

Fig. 3. Anisotropy (in black) of the critical current $j_c(0°)/j_c(90°)$, as determined from the flux fronts of Fig. 2a, versus the externally applied magnetic field. For small penetration distance $d(\alpha)$, the anisotropy cannot be determined accurately, as indicated by the error bars. For large applied fields, the anisotropy approaches $j_c(0°)/j_c(90°) = 1.30(5)$.

4. Model

We now discuss a simple geometrical model based on the channeling of vortices that reproduces our observations. This model closely resembles that of Pannetier et al. [1], but the

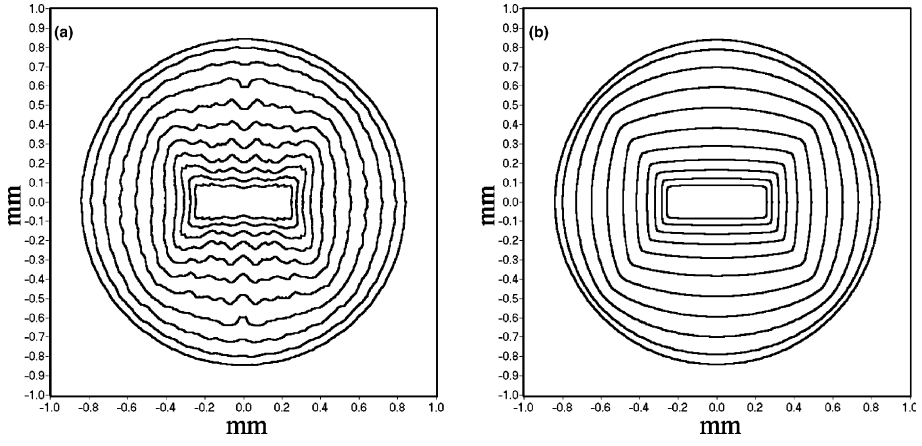

Fig. 2. (a) Measured flux fronts starting at $\mu_0 H_z = 9.5$ mT applied field (largest circle). Indicated are consecutive fronts separated by field steps of 4.5 mT. Upon increasing $\mu_0 H_z$, the front advances into the sample and we observed a transformation from a circular to a rectangular shape. (b) Fronts calculated from a simple geometrical model (see text) based on flux channeling along anti-dot rows.

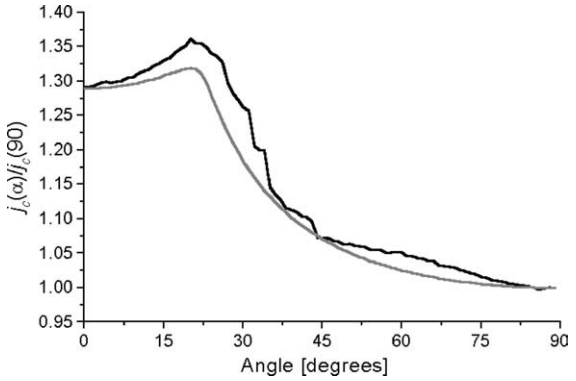

Fig. 4. Normalized angular dependence of the critical current density. The experimental result at an applied field of 50 mT is shown by the black curve; the corresponding anisotropy j_c (0°)/j_c (90 °) is 1.30(5). The simple geometrical model (see text) gives the result shown by the light gray curve. The experimental peak at $\alpha = 20°$ is due to repulsion between vortices on meeting flux channels, slowing down the flux penetration. This effect is not incorporated in our model.

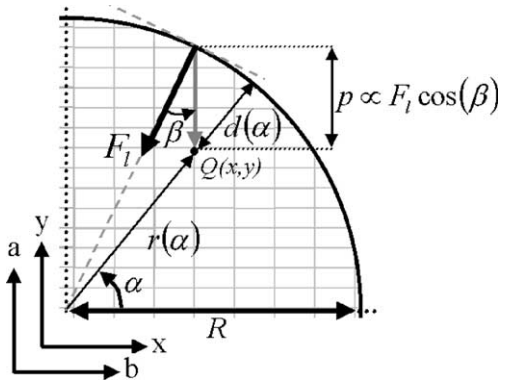

Fig. 5. Schematic representation of the first quadrant of the sample. The rectangular anti-dot array is shown in light gray. F_l is the Lorentz force, the dark gray arrow indicates its projection $F_l \cos(\beta)$ along the closest anti-dot lattice vector. The penetration distance p along the channel is proportional to this projection and the applied field (see text).

channeling of vortices is incorporated in a more straightforward manner. As discussed above, flux penetration takes place from the sample edge, where the flux moves into the channel most parallel to the Lorentz force. With increasing applied magnetic field, vortices move further inward along the anti-dot channels. Since the vortices are constrained to the channels, they move inside under the influence of the *projection* of the Lorentz force F_l along the channel direction (see Fig. 5).

The theoretical shape of the flux front generated by the flux penetration along e.g. the a-direction is described by an ellipse, as we will now show. The projection of the Lorentz force along a channel is proportional to $F_l \cos\beta$ (see Fig. 5). We sum the Lorentz force over the total width of the current carrying band. Because of current continuity, the total Lorentz force F_l is not dependent on the polar angle α. Hence we take the penetration distance p along a channel proportional to $F_l \cos\beta$, since the total pinning force (that balances the total Lorentz force along a channel) is linear in penetration distance.

With an anisotropy A and sample radius R, the y-coordinate of an arbitrary point $Q(x,y)$ on the flux front due to channeling along the a-direction is:

$$y = \sqrt{R^2 - x^2} - AF_l \cos(\beta) = \sqrt{R^2 - x^2}(1 - C), \quad (1)$$

where $C = (AF_l)/R$ is proportional to the externally applied field. Clearly Q is on an ellipse with increasing eccentricity for increasing field ($C \to 1$). The proportionality constant is different along the a- and b-anti-dot lattice vectors (due to the different number of anti-dots per unit length). Hence the flux penetration is governed by two ellipses with major axes turned by 90°. The actual front is given by the minimum distance from the center of the sample to those two ellipses. To make the anisotropy more explicit we write the equations for the ellipses in polar coordinates:

$$r_q(\alpha) = \sqrt{\frac{R^2(1 - C_q)^2}{(1 - C_q)^2 \cos^2\left(\alpha - q\frac{\pi}{2}\right) + \sin^2\left(\alpha + q\frac{\pi}{2}\right)}}, \quad (2)$$

where we replaced C by C_q, with q zero or one for vortices channeling along the a- or b-lattice vector respectively and $C_0 = pA/R$ and $C_1 = p/R$. The intersection of these two ellipses defines the point where flux entering from two perpendicular channels meets. The position of this intersection is related to the anisotropy A. Since this point can be easily identified in the experiment, we now derive

an analytical expression for its position. When p in our model equals R/A, the flux penetration along the a-lattice vector stops, and the flux front coincides with the x-axis. The point of intersection with the other ellipse then lies on the x-axis. It is easily seen that this is at $x_0 = R(1 - A^{-1})$. In our experiment, we find that the intersection points at all applied fields are on a line (ending in $(x_0, 0)$) with an angle of $\gamma_{\text{exp}} \cong 54(5)^\circ$ with respect to the x-axis. Experimentally we find $x_0 = 0.23(1)R$. From our model, the line is not absolutely straight, but the angle γ is only weakly dependent upon p. We find for this angle $\gamma_{\text{theory}} \cong \arctan((2A-1)^{1/2}) \cong 52(1)^\circ$ for our experimental value of A. To include the interaction between horizontal and vertical channels, we use an interaction term V as previously proposed by Pannetier et al. [1]. Thus we obtain:

$$r(\alpha) = \frac{r_0 + r_1 - \sqrt{(r_0 - r_1)^2 - 4V^2}}{2}. \quad (3)$$

In Fig. 2, we compare our experimentally obtained fronts (Fig. 2a) with Eq. (3) (Fig. 2b), where we used the experimentally determined anisotropy 1.30(5) and a small value for the interaction: $V = 0.013$. The nice correspondence shows that our simple model describes all the main features of the fronts in an excellent manner.

5. Summary

We investigate the flux penetration in a YBCO thin film with circular geometry and perforated with a rectangular (1:2) array of anti-dots. We show that the flux penetration pattern changes from circular to rectangular, reflecting the influence of the underlying anti-dot lattice. Preferential flux penetration along the main anti-dot lattice vectors (a and b) is observed, caused by channeling of vortices along rows of anti-dots. We determine the angular dependence of the normalized critical current $j_c(\alpha)$. We find that with increasing field the anisotropy $A = j_c(0^\circ)/j_c(90^\circ)$ increases to $A = 1.30(5)$. This value is much smaller than the value ~ 60 found in simulations [5]. The discrepancy can be ascribed to a large difference between anti-dot size and spacing as well as by switching between channels.

Finally, we present a model based on the observation that vortices move from the sample edge only along the anti-dot lattice vectors. This model reproduces very well the shape of the experimental flux fronts and other features.

Acknowledgements

This work was supported by FOM (Stichting voor Fundamenteel Onderzoek der Materie), which is financially supported by NWO (Nederlandse Organisatie voor Wetenschappelijk Onderzoek). We also acknowledge the ESF (European Science Foundation) VORTEX Program for support.

References

[1] M. Pannetier, R.J. Wijngaarden, I. Fløan, J. Rector, B. Dam, R. Griessen, P. Lahl, R. Wördenweber, Phys. Rev. B 67 (2003) 212501.
[2] R. Wördenweber, A.M. Castellanos, P. Selders, Physica C 332 (2000) 27.
[3] S. Koleśnik, V. Vlasko-Vlasov, U. Welp, G.W. Crabtree, T. Piotrowski, J. Wróbel, A. Klimov, P. Przystupski, T. Skośkiewicz, B. Dabrowski, Physica C 341 (2000) 1093.
[4] V. Vlasko-Vlasov, U. Welp, V. Metlushko, G.W. Crabtree, Physica C 341 (2000) 1281.
[5] C. Reichhardt, G.T. Zimányi, N. Grønbech-Jensen, Phys. Rev. B 64 (2000) 014501.
[6] M. Baert, V.V. Metlushko, R. Jonckheere, V.V. Moshchalkov, Y. Bruynseraede, Phys. Rev. Lett. 74 (1995) 3269; L. Van Look, B.Y. Zhu, R. Jonckheere, B.R. Zhao, Z.X. Zhao, V.V. Moshchalkov, Phys. Rev. B 66 (2002) 214511.
[7] M. Vélez, D. Jaque, J.I. Martín, M.I. Montero, Ivan K. Schuller, J.L. Vicent, Phys. Rev. B 65 (2002) 104511.
[8] B. Dam, J.M. Huijbregtse, F.C. Klaassen, R.C.F. van der Geest, G. Doornbos, J.H. Rector, A.M. Testa, S. Freisem, J. Aarts, J.C. Martinez, B. Stäuble-Pümpin, R. Griessen, Nature 399 (1999) 439.
[9] R.J. Wijngaarden, K. Heeck, M. Welling, R. Limburg, M. Pannetier, K. van Zetten, V.L.G. Roorda, A.R. Voorwinden, Rev. Sci. Instr. 72 (2001) 2661.